ORIGINAL PAPER

V M
VIA MEDICA

Application of adipose mesenchymal stem cell-derived exosomes-loaded β-chitin nanofiber hydrogel for wound healing

Ying Liu[1,2], Yunen Liu[3,4], Yan Zhao[5], Mi Wu[4], Shun Mao[4], Peifang Cong[2], Rufei Zou[5], Mingxiao Hou[3,4], Hongxu Jin[2*], Yongli Bao[1*]

[1]National Engineering Laboratory for Druggable Gene and Protein Screening, Northeast Normal University, Changchun, China

[2]Emergency Medicine Department of General Hospital of Northern Theater Command, Laboratory of Rescue Center of Severe Wound and Trauma PLA, Shenyang, China

[3]Shenyang Medical College, Shenyang, China

[4]The Second Affiliated Hospital of Shenyang Medical College, the Veterans General Hospital of Liaoning Province, Shenyang, China

[5]Jihua Laboratory, Foshan, China

Abstract

Introduction. Clarifying the role and mechanism of exosome gel in wound repair can provide a new effective strategy for wound treatment.

Materials and methods. The cellular responses of adipose mesenchymal stem cell-derived exosomes (AMSC-exos) and the wound healing ability of AMSC-exos-loaded β-chitin nanofiber (β-ChNF) hydrogel were studied *in vitro* in mouse fibroblasts cells (L929) and *in vivo* in rat skin injury model. The transcriptome and proteome of rat skin were studied with the use of sequenator and LC-MS/MS, respectively.

Results. 80 and 160 μg/mL AMSC-exos could promote the proliferation and migration of mouse fibroblastic cells. Furthermore, AMSC-exos-loaded β-ChNF hydrogel resulted in a significant acceleration rate of wound closure, notably, acceleration of re-epithelialization, and increased collagen expression based on the rat full-thickness skin injury model. The transcriptomics and proteomics studies revealed the changes of the expression of 18 genes, 516 transcripts and 250 proteins. The metabolic pathways, tight junction, NF-κB signaling pathways were enriched in Kyoto Encyclopedia of Genes and Genomes (KEGG) Pathway. Complement factor D (CFD) and downstream Aldolase A (Aldoa) and Actn2 proteins in rats treated with AMSC-exos-loaded β-ChNF hydrogel were noticed and further confirmed by ELISA and Western blot.

Conclusion. These findings suggested that AMSC-exos-loaded β-ChNF hydrogel could promote wound healing with the mechanism which is related to the effect of AMSC-exos on CFD and downstream proteins. *(Folia Histochemica et Cytobiologica 2022, Vol. 60, No. 2, 167–178)*

Keywords: Adipose mesenchymal stem cell-derived exosomes; β-chitin nanofiber; rat skin; wound healing; transcriptomics; proteomics

*Correspondence address: Yongli Bao
National Engineering Laboratory for Druggable Gene and Protein Screening, Northeast Normal University, 2555 Jingyue Street, Changchun 130117, China
phone: +86-431-89165920
e-mail: baoyl800@nenu.edu.cn

*Correspondence address: Hongxu Jin
General Hospital of Northern Theater Command, 83 Wenhua Road, Shenyang, 110016, China phone: +86-24-28851293
e-mail: cszx_jhx@163.com

Introduction

Skin is the body's important barrier against external damage. When a wound is caused, it substantially reduces the life quality of patients, and brings a great economic burden and the society [1, 2]. Recently, several studies on the roles of mesenchymal stem cell-derived exosomes (MSC-exos) in wound healing have shown that MSC-exos can activate certain signaling pathways to regulate growth factors as well as the proliferation and migration of cells [3–5]. However, there are challenges in the application of MSC-exos owing to the rapid clearance by the innate immune system. Injury repair is a kind of complex multiphase process, while the inevitably rapid clearance of free exosomes in vivo leads to low effectiveness and efficiency of this therapeutic [6]. The combination of exosomes with biomaterials can extend the retention time of exosomes on the wound surface without affecting their biological activity [7, 8]. There is an urgent need to find better ways to employ MSC-exos. The hydrogel can provide a wet healing environment, and act as a carrier for exosomes to promote wound healing. It has been reported that exosomes-loaded chitosan hydrogel can promote wound healing [9, 10]. While chitin-based biomaterials have good biological activity and have been widely applied in damage repair, few studies have investigated the treatment effects of MSC-exos-loaded β-chitin nanofibers (β-ChNF) hydrogel on wounds, and the mechanism remains unclear [11]. We speculated that incorporating exosomes with β-ChNF hydrogel would provide enhanced beneficial effects on wound healing. The adipose mesenchymal stem cells are easy to obtain and their exosomes have been reported to play a beneficial role in damage repair [12].

Therefore, the main aim of this study was to investigate the effect of adipose mesenchymal stem cell-derived exosomes (AMSC-exos)-loaded β-ChNF hydrogel on wound healing. Furthermore, the mechanism of AMSC-exos-loaded β-ChNF hydrogel was detected based on transcriptomics and proteomics. The results will improve the understanding of wounds, and provide a biological basis for possible clinical applications of AMSC-exos for wound healing.

Materials and methods

Materials. The exosomes derived from adipose mesenchymal stem cells were provided by Rengen Biosciences (lot#201104, Liaoning, China). The adipose mesenchymal stem cells were extracted from the groin adipose tissue of male C57BL/6 mice. The scanning and transmission electron microscopy, nanoparticle tracking analysis, Western blot and ELISA results of AMSC-exos were performed as the instructions of the manufacturers. L929 mouse fibroblast cells (derived from normal subcutaneous areolar and adipose tissue of a 100-day-old male C3H/An mouse) were purchased from the Institute of Biochemistry and Cell Biology (Shanghai, China). They were cultured in DMEM medium (Gibco, USA), and 15% fetal bovine serum (HyClone, USA), 100 U/mL penicillin and 100 μg/mL streptomycin (Beyotime Biotechnology, China) were added. Squid pens were obtained from a local fish market, China. Hydrochloric acid and sodium hydroxide were purchased from Sinopharm Chemical Reagent Co., Ltd., China.

Cell proliferation assay. The L929 cells were seeded into in 96-well plates for 24 h, and then treated with various concentrations of AMSC-exos (40, 80 and 160 μg/mL) for 6, 12 and 24 h. After that, 10 μL of CCK8 was added and cells were incubated for 3 h. The absorbance was measured at 570 nm by a microplate reader. The experiment was repeated three times. The cell proliferation was expressed as the mean ± SD of the absorbance ratio of the AMSC-exos treated cells to the untreated cells.

Scratch wound healing and transwell assays. When the L929 cells reached 90% confluence in 6-well plates, scratch wound healing was conducted. Briefly, a straight line at the bottom of the 6-well plate was made using a pipette tip, and then phosphate-buffered saline (PBS) was used to wash out the cell debris. Finally, AMSC-exos (40, 80 and 160 μg/mL) were used to treat the cells, and the images of cells were taken at 0 h, 12 h, 24 h and 36 h. Cell scratch test was repeated three times.

During the cell migration assays, L929 cells in a serum-free culture medium were added to the upper chambers, while the lower chambers were added with a medium supplemented with 20% fetal bovine serum. AMSC-exos (40, 80 and 160 μg/mL) were added to the upper chamber and the cells were incubated for 24 hours. After that, unmigrated cells were swabbed, and 0.05% crystal violet solution was used for staining. The transwell assay was repeated three times.

Preparation of adipose mesenchymal stem cell-derived exosomes (AMSC-exos) loaded β-chitin nanofiber (β-ChNF) hydrogel. After washing and drying, the squid pen was treated with 0.1 mol/L hydrochloric acid (Sinopharm Chemical Reagent Co., Ltd., China) and 4% (wt/vol) sodium hydroxide (Sinopharm Chemical Reagent Co., Ltd., China) to finish demineralization and deproteinization. Ultrasonic homogenizer (Scientz JY92-IIDN, China) was used to form β-ChNF hydrogel. The β-ChNF hydrogel obtained was added with AMSC-exos (200 μg/mL), and the hydrogel and AMSC-exos were homogenized to form AMSC-exos-loaded β-ChNF hydrogel.

Establishment of rat model. Sprague-Dawley rats (male, 6–8 weeks old) were purchased from Liaoning Changsheng biotechnology co., Ltd (China). After acclimatization, all rats were randomly divided into the control, hydrogel, exosomes, and exosomes hydrogel groups (n = 6 in each group). All animals were anesthetized and created circular full-thickness cutaneous wounds at the dorsal skin with a circular mold. At 0, 3, 5, 6, 7, 8, 10 and 12 days after the operation, the rats were carefully observed. The rats in hydrogel and exosomes hydrogel groups were treated with 400 μL hydrogel or exosomes hydrogel, and each rat of the exosomes group was treated with 80 μg exosomes just after the operation. The wound healing rate of each rat was measured with Image J (Nation Institutes of Health, USA) and calculated as follows: wound healing rate (%) = (A0-At)/ A0 × 100%. The animal welfare and experimental design were approved by the Ethics Committee of the General Hospital of Northern Theater Command, Shenyang, China.

Histological examinations. The skin samples of rats were harvested and fixed by 10% formaldehyde. After being embedded in paraffin blocks using the Leica Microsystem tissue processor (ASP300S, Germany), sections of 5 μm thickness were sliced using a Leica Microsystem microtome (Model RM 2265, Germany), and hematoxylin and eosin (HE) staining and Masson staining were conducted according to the instructions. The images were taken using an Image J software to detect the percentage of the collagen staining area (blue) in the total area for Masson staining results. The full-thickness of wounds in each group was measured.

Transcriptomics. Eight days later, animals were sacrificed and skin tissue was collected. RNA extraction and library construction were conducted. Then the cleaved RNA fragments were reverse-transcribed to create the cDNA, which was next used to synthesize U-labeled second-stranded DNAs with E. coli DNA polymerase I RNase H and dUTP. After the heat-labile UDG enzyme treatment of the U-labeled second-stranded DNAs, the ligated products are amplified with PCR by the following conditions: initial denaturation at 98°C for 30 min; 14 cycles of denaturation at 98°C for 15 sec, anealing at 60°C for 30 sec, and extension at 72°C for 30 sec; and then final extension at 72°C for 5 min. The average insert size for the final cDNA library was 350 bp (± 50 bp). At last, we performed the paired-end sequencing on an Illumina Hiseq X-Ten (LC Bio , China).

Proteomics. The TMT marker-ed peptides were dissolved in 0.1% formic acid (solvent A) and loaded onto a reversed-phase analytical column (Thermo scientific EASY column, C18, 75 μm*150 mm, 3 μm). Liquid phase gradient setting: 0–2 min, 2–8% B; 2–42 min, 8–30% B; 42–49 min, 30–45% B; 49–50 min, 45–100% B; 50–60 min, 100% B. Solvent A contained 0.1% formic acid in water; Solvent B contained 0.1% formic acid in 95% acetonitrile. All were at a constant flow rate of 300 nL/min on an Easy nLC 1200 UPLC system. The Q-Ex -Active HF-X mass spectrometer was used for data-dependent acquisition. The distribution of peptide length identified by MS/MS was in accordance with the quality control requirements.

Bioinformatics analysis. The sequence quality was verified using FastQC (http://www.bioinformatics.babraham.ac.uk/projects/fastqc/). We used Hisat2 to map reads to the mouse genome GRCm38 in Ensemble92. The mapped reads of each sample were assembled using StringTie. UniProt-GOA database (www. http://www.ebi.ac.uk/GOA/) was used to conduct Gene Ontology (GO) annotation; The annotated protein pathway was conducted by Kyoto Encyclopedia of Genes and Genomes (KEGG) database. Differentially expressed protein databases were searched against the STRING database for protein-protein interactions.

ELISA. The ELISA kit was purchased from Shanghai Jianglai Biotechnology Co., Ltd (Shanghai, China) to detect the expression of CFD in cell homogenates. After homogenization in PBS (0.02 mol/L, pH 7.0) and centrifugation at 5000, for 10 min, the supernatant was collected. Standard and sample were added and then the measurements were performed according to manufacturer's instruction. OD value was measured at 450 nm wavelength.

Western blot. After the protein extraction, antibody incubation was performed. The primary antibody included Alpha-actinin-2 (Actn2, 1:1000, 14221-1-AP, Proteintech, USA), Aldolase A (Aldoa, 1:1000, 11217-1-AP, Proteintech, USA), Glyceraldehyde 3-phosphate dehydrogenase (GAPDH, 1:1000, 2118, Cell Signaling Technology, Boston, USA) and anti-rabbit secondary antibody (1:2000, ab6721, Abcam, UK). A Tanon 5200 Full automatic chemiluminescence image analysis system (Tanon Science and Technology Co. Ltd., Shanghai, China) was used for proteins' visualizing.

Statistical analysis. All data were analyzed with SPSS 22.0 (IBM, Amrok, NY, USA). Quantitative data were expressed as mean ± standard deviation. The two-tailed paired Student's t-test was used for two groups comparisons. Comparison between multiple groups was performed by one-way ANOVA. The difference was statistically significant at $P < 0.05$.

Results

AMSC-exos boost the proliferation of L929 cell
CCK8 was conducted to test the effects of AMSC-exos on cell proliferation. As presented in Fig. 1a, 40 μg//mL had no significant effect on L929 cell proliferation, while it was increased notably when the cells
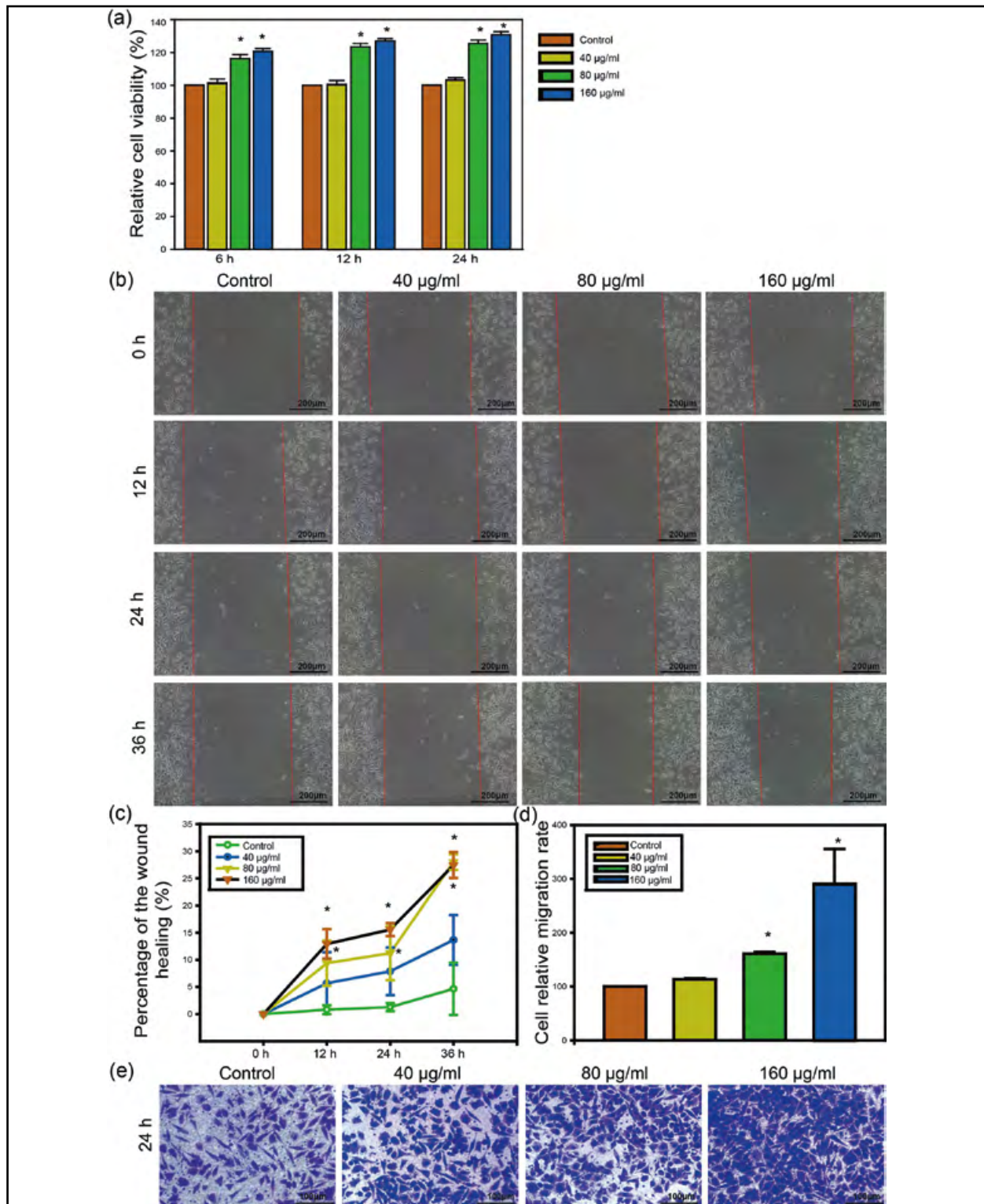
Figure 1. Adipose mesenchymal stem cell-derived exosomes (AMSC-exos) boosts the proliferation and migration of L929 cells; **(a)** AMSC-exos effects on cells proliferation were assessed by CCK8 test as described in Methods; **(b, c)** The scratch assay results of cell migration; **(d, e)** The transwell assay results of cell migration. Data present means ± SD of at least 3 independent experiments. * P < 0.05 as compared with the control group.

were exposed to AMSC-exos for 6 h, 12 h and 24 h at 80 and 160 µg/mL (P < 0.05). As fibroblasts' migration played an important role in the wound healing process, scratch and transwell assays were conducted to test cell migration. As can be seen from Fig. 1b of the scratch assay, the wound (scratch) areas of the treated groups were all smaller than that of the untreated group at a certain time, indicating that L929 fibroblasts treated with 80 and 160 µg/mL AMSC-exos for 12 h, 24 h and 36 h migrated faster. Especially, after treating with 80 and 160 µg/mL AMSC-exos, the percentage of the wound healing reached 26.9–29.7% and 24.9–29.7%, respectively, while the untreated group was 8.8–18.0% (Fig. 1c). During the transwell assay, it was shown that more L929 cells (treated with 80 and 160 µg/mL AMSC-exos) migrated to the lower surface of the membrane, compared with the L929 control cells (Fig. 1d,e; P < 0.05). Moreover, 80 and 160 µg/mL AMSC-exos enhanced the migration up to 157.8–164.3% and 218.3–342.4%, respectively, indicating a significant migration enhancement effect (P < 0.05) compared with the untreated group. Both the scratch wound healing and transwell assays confirmed the promotion of migration of fibroblasts induced by exposure of AMSC-exos.

Effect of AMSC-exos-loaded β- ChNF hydrogel on wound healing

As shown in Fig. 2, the scanning electron microscopy of hydrogel and AMSC-exos hydrogel showed that the hydrogels were porous structure (Fig. 2a) and exosomes were distributed in its pores (Fig. 2b). After treatment with AMSC-exos hydrogel, the wound areas of rat skins were observed and taken pictures on day 0, 3, 5, 6, 7, 8, 10, 12, some representative pictures were presented in Fig. 2c. It was clearly visible that the wound areas in the exosomes hydrogel group were much smaller than that in the model group, and they were almost healed on day 12 while the wound in the model group was still apparent. Wound areas were measured and the wound healing rates were plotted against days after the operation, as shown in Fig. 2d. From day 3 to day 12, the wound healing rate in the exosomes hydrogel group increased from 16.6% to 95.2%, which was significantly faster than that in the model group (from 4.7% to 79.3%) (P < 0.05). In conclusion, AMSC-exos hydrogel noticeably increased wound closure in rats. Modified Masson staining showed that the amount of collagen deposited was markedly higher in the exosomes hydrogel group than in the model, hydrogel and exosomes groups at day 12. The collagen areas were increased after AMSC-exos hydrogel treatment (Fig. 2e, f). These data suggested that the AMSC-exos

hydrogel accelerated wound healing in rats. The HE staining of rats' skins with wound regions was shown in Fig. 2g. The cellular debris, necrotic tissue, and little regeneration of the epidermis were observed in the model group of rats. Nevertheless, most of the debris and necrotic tissue were cleared, and a more integrated epidermis was regenerated in rat treated with the hydrogel, exosomes or exosomes-hydrogel. It was noted that in the exosomes-hydrogel group, the hair follicles, blood vessels, and other skin appendages were substantially increased.

Transcriptome analysis of the effect of AMSC-exos--loaded β-ChNF hydrogel on wound

To gain a more comprehensive insight into the gene expression changes of AMSC-exos intervention, transcriptome analyses were performed. A great deal of 35536 genes, including 32883 known genes (21584 expressed) and 2653 new genes were analyzed; among those, 18 genes were differentially expressed following AMSC-exos hydrogel (Tab. 1); 7 genes were increased, while 11 genes were reduced (DESeq2, FDR < 0.05, $|\log_2 \text{FoldChange}| > = 1.00$). The number of transcripts is 62 993, including 41078 known transcripts (27362 expressed) and 21915 new transcripts; among those, 516 transcripts were differentially expressed following AMSC-exos hydrogel treatment. The expression of 250 transcripts was increased, while 266 ones was reduced (DESeq2, FDR < 0.05, $|\log_2 \text{FoldChange}| > = 1.00$). The overall distribution of the differentially expressed transcripts was shown by the volcano map and heatmap (Suppl. Fig. 1). Go function enrichment histogram of significantly different transcripts was shown in Suppl. Fig. 2. Among biological process (BP) classes, the mRNAs involved in nitrogen compound transport, regulation of cytokinesis, positive regulation of coagulation and others were identified in response to the treatment. In the cellular component (CC) category, the genes expressed were mostly enriched for ATP−binding cassette transporter complex, actin cap, cortical actin cytoskeleton and mitochondrial intermembrane space protein transporter complex. Finally, in molecular function (MF) classes, keratin filament binding and intermediate filament binding were the top two enriched terms. Additionally, ATP binding, alcohol dehydrogenase [NAD(P)+] activity and UDP−activated nucleotide receptor activity suggested an active energy metabolism in wound healing. Next, the biological functions were further studied by KEGG pathway enrichment. Surprisingly, two metabolism-associated pathways were identified, including inositol phosphate metabolism and selenocompound metabolism (Suppl. Fig. 3a). Moreover, the distribution of significantly
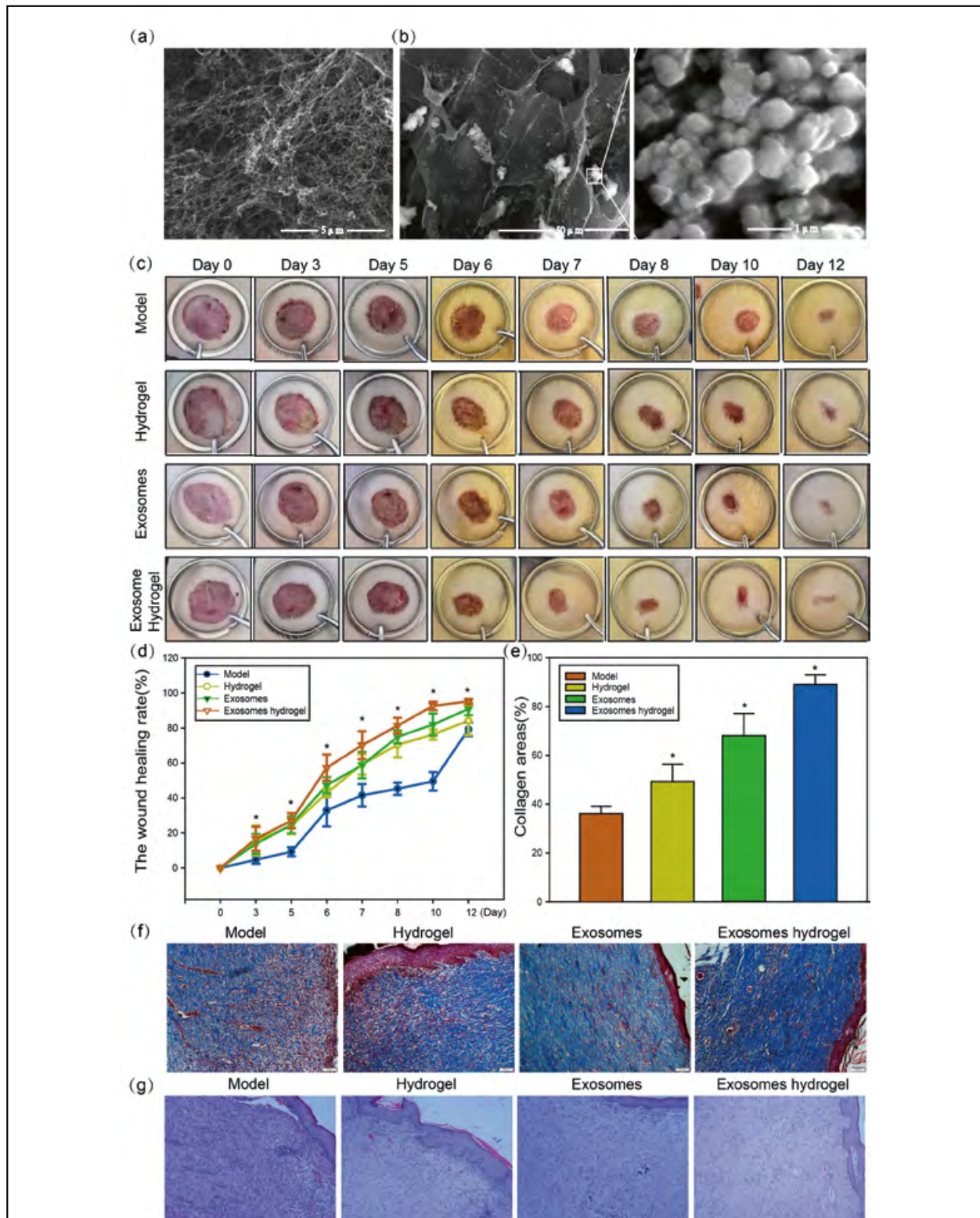
Figure 2. Adipose mesenchymal stem cell-derived exosomes (AMSC-exos) hydrogel increased the wound healing rate in rats; **(a, b)** The SEM photographs of chitin hydrogel with AMSC-exos were provided by the exosomes' manufacturer; **(c)** Photographs of wounds closure from 0 to 12 d after surgery; **(d)** The wound healing rate of full-thickness wounds for each treatment group; **(e)** Collagen deposition of the full-thickness wounds in each group. Image J software was used to detect the percentage of the collagen staining area (blue) in relation to the total area; **(f)** Representative microphotographs of the wounds' sections stained with modified Masson method in each group; **(g)** Representative microphotographs of the wounds' sections stained with HE in each group. Data present means ± SD of at least 3 independent experiments. *$P < 0.05$ as compared with model group (control).

Table 1. Transcriptomics revealed the significantly different genes of the treatment group vs. model (control) group in rats

Gene ID	T_P-value	Protein ID	Gene name
ENSRNOG00000002767	0.015598861	Q62936	Dlg3
ENSRNOG00000007172	0.02045685	Q99JP0	Map4k3
ENSRNOG00000007765	2.39E-10	P97401	Frzb
ENSRNOG00000010649	0.009832254	O35927	Ctnnd2
ENSRNOG00000011892	0.001116417	Q8K415	Slc36a2
ENSRNOG00000014090	0.001116417	Q8VHE9	Retsat
ENSRNOG00000015354	0.003394701	Q9Z0U5	Aox1
ENSRNOG00000016460	0.002198257	P05371	Clu
ENSRNOG00000020380	0.043452089	P97590	Lgals7
ENSRNOG00000022946	0.014624121	O88446	Slc22a3
ENSRNOG00000026371	0.022547337	Q6IFU8	Krt17
ENSRNOG00000033564	0.007183107	P32038	Cfd
ENSRNOG00000033933	0.000232522	P01039	Csta
ENSRNOG00000045548	7.16E-05	Q3TCT4	Entpd7
ENSRNOG00000050420	2.95E-05	Q6P6Q2	Krt5
ENSRNOG00000053118	1.15E-13	Q6P5E6	Gga2
ENSRNOG00000055850	4.07E-12	O43143	DHX15
ENSRNOG00000056651	7.80E-14	—	—

different transcripts in the ipath integration pathway was also shown (Suppl. Fig. 3b).

Quantitative proteomic analysis of the effect of AMSC-exos-loaded β-ChNF hydrogel on wound

For global proteome analysis, the fold-change cutoff was set at 1.2 (treatment *vs.* model); we identified 4160 proteins in wound tissues. Among these, 169 proteins were up-regulated, and 81 proteins were down-regulated as compared to the model (Suppl. Fig. 4a). Protein cluster analysis results were also proceeded (Suppl. Fig. 4b). Differentially expressed proteins were analyzed by Gene Ontology. From BP, CC and MF results, the biological roles of proteins were explained in Fig. 3a. In the BP category, the up-regulated proteins were highly enriched in terms such as muscle system process, muscle contraction and muscle structure development. The enrichment analysis of the CC category revealed proteins related to supramolecular fibers, cytoplasmic proteins and other. According to the MF enrichment results, we found that the differentially expressed proteins are taking part in cytoskeletal protein binding and other proteins' binding (Fig. 3b–d). Metabolism, genetic information processing, environmental information processing, cellular processes and body's system changes were enriched in KEGG Pathway (Suppl. Fig. 5a). The representative protein interaction

networks of tight junctions was also shown (Suppl. Fig. 5a).

Combined analysis and validation of the different proteins

The combined analysis results demonstrated that the proteins exhibited the same trends as the expression of genes. The overall gene/protein comparison between transcriptome and proteome is shown in Fig. 4a; the significantly different gene/protein comparison between transcriptome and proteome was shown in Fig. 4b. Common differential gene/protein complement factor D (CFD) were found according to the gene/protein conjoint analysis results, which were further proved by ELISA results (Fig. 4c). According to the protein PPI network, we also paid attention to the change of Actn2 and Aldoa. These two proteins were further proved by Western blot in rats (Fig. 4d). Aldoa protein is related to cell metabolism. To prove that exosomes can increase the expression of Aldoa protein to promote cell proliferation during wound healing, we detected the expression of CFD and Aloda proteins in exosomes-treated L929 cells. ELISA and Western blotting results showed that the expression of CFD was decreased and downstream Aldoa protein was increased in L929 cells after exosome intervention (Fig. 4e).
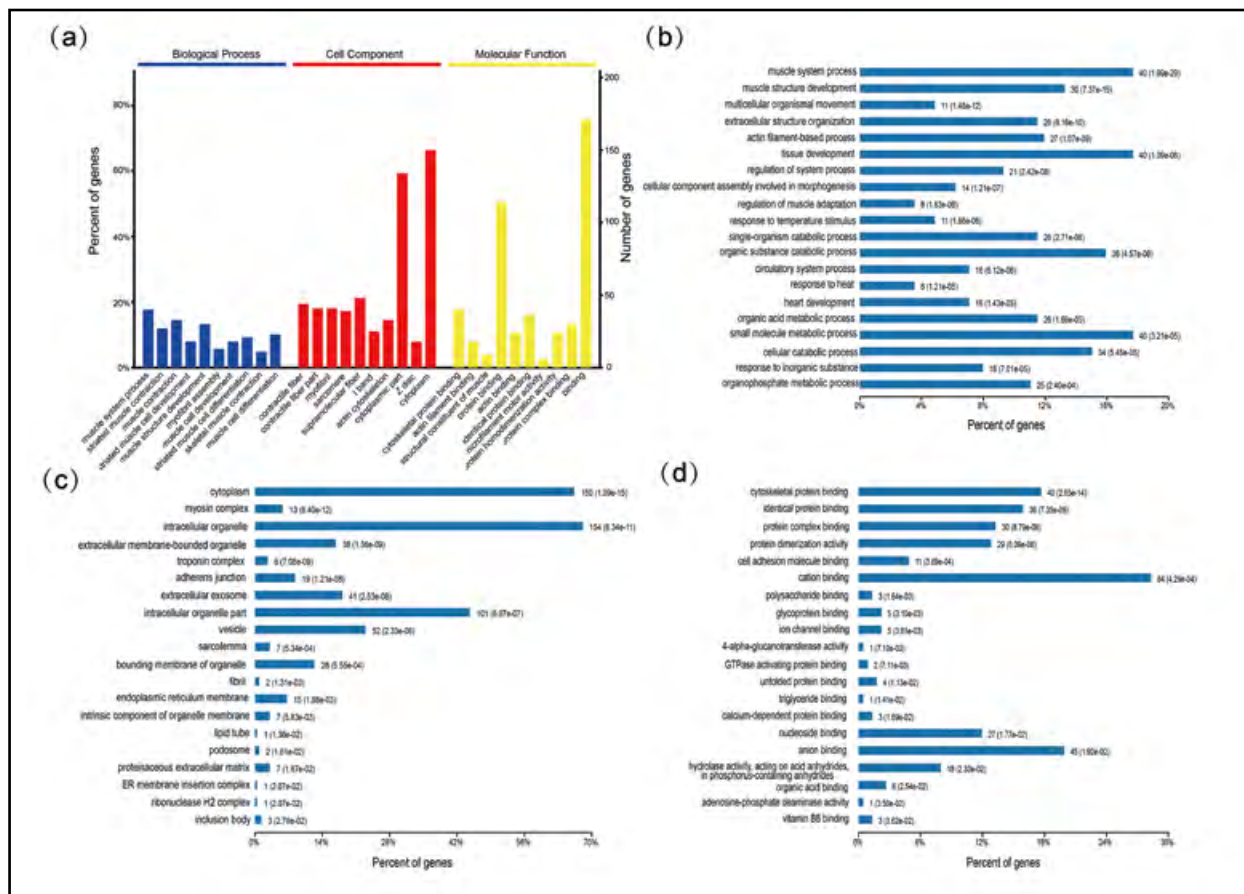
Figure 3. Adipose mesenchymal stem cell-derived exosomes (AMSC-exos) hydrogels affected the expression of cellular regulatory proteins based on proteomics analysis; **(a)** GO functional annotation bar chart of significantly different proteins; **(b)** biological process analysis of different proteins; **(c)** cellular component analysis of different proteins; **(d)** molecular function analysis of different proteins.

Discussion

Wound healing requires cellular repair through a series of complex signaling pathways including hemostasis, inflammation, proliferation and maturation [13]. During the proliferation phase, the fibroblasts will be recruited from the wound borders and massively proliferated [14]. The fibroblasts can differentiate into myofibroblasts to contract the wound, and release lots of collagen to fill the wound bed. The fibroblasts play an important role in wound healing and accelerating the proliferation of fibroblasts is beneficial to wound healing [15, 16]. Therefore, L929 mouse fibroblast cells, which have often been used in wound healing studies, were used to prove the effect of AMSC--exos on wound healing. L929 cells are adherent cells with strong proliferation and passage ability, which could meet the requirements of proliferation and migration experiments *in vitro* [17, 18]. MSC-exos are rich in a variety of proteins, mRNAs and cytokines. It was reported that MSC-exos could promote the

proliferative and migratory abilities of cells and thus accelerate wound healing [19–21]. However, the effect of AMSC-exos on skin fibroblasts is not very clear. To evaluate the effect of AMSC-exos on fibroblasts migration, scratch wound healing assay and transwell migration assay were used in this study. A considerable increase in fibroblast proliferation and migration was noticed on cells treated with AMSC-exos 80 or 160 μg/mL, when compared with control. However, there was no significant changes in the proliferation and migration of fibroblasts after the dose of 40 μg//mL AMSC-exos intervention. These results enriched the understanding of the effects of AMSC-exos on fibroblasts and provided a theoretical basis for further study on promoting wound healing.

AMSC-exos was loaded in β-ChNF hydrogel in order to solve the problem that AMSC-exos local fixed storage ability was poor during wound healing [22]. Chitin nanofibers hydrogel is a good carrier for sustained-release materials such as nanoparticles or exosomes. Chitin hydrogel could notably increase the stability of proteins and microRNAs in exosomes, as
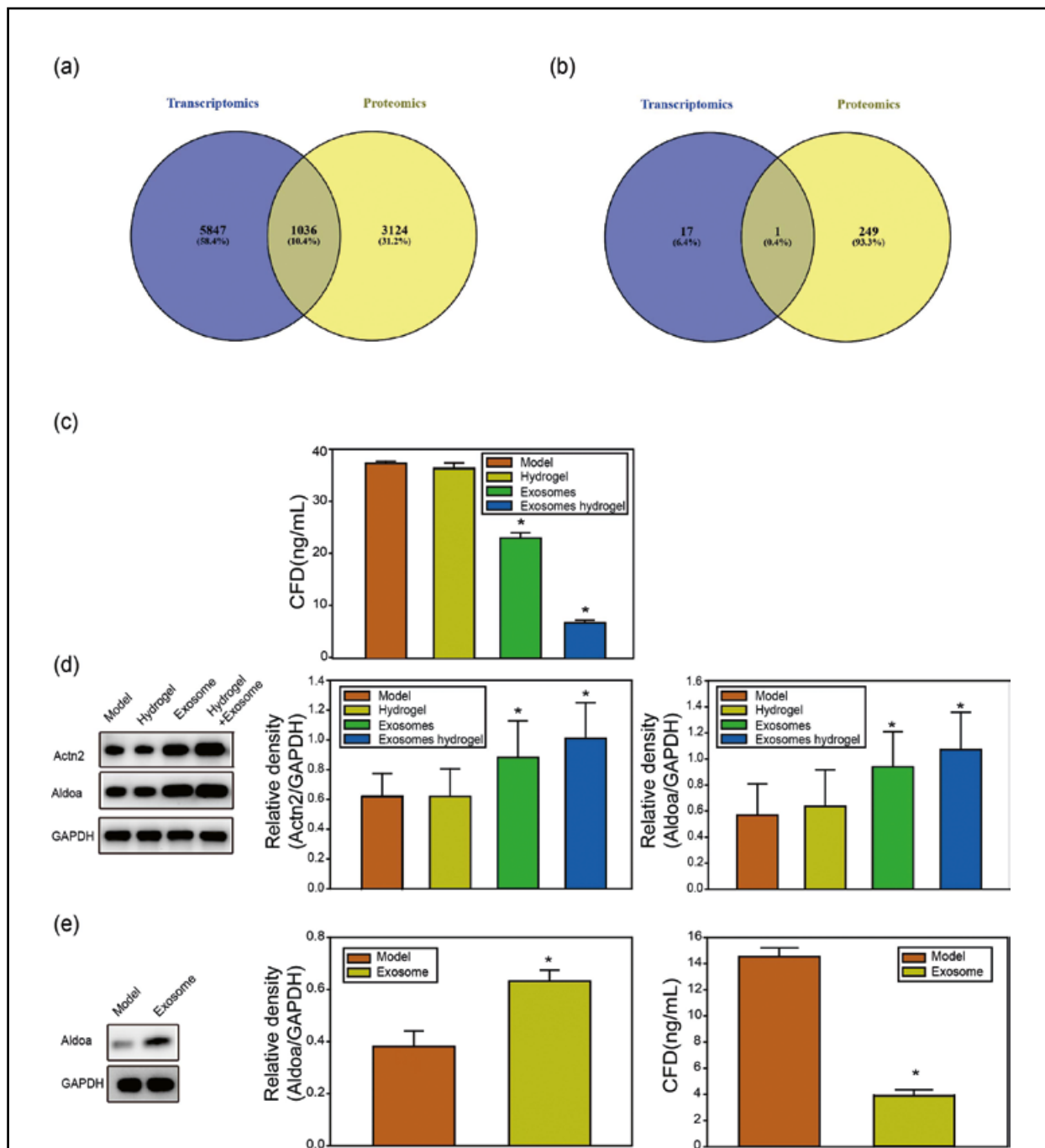
Figure 4. Complement Factor D (CFD), alpha-actinin-2 (Actn2) and aldolase A (Aldoa) proteins changes were found in rat skin after adipose mesenchymal stem cell-derived exosomes hydrogel (AMSC-exos) treatment; **(a)** Venn diagram of overall gene/protein comparison between transcriptome and proteome; **(b)** Venn diagram of significantly different gene/protein comparisons between transcriptome and proteome; **(c)** Expression of CFD protein in rat skin; **(d)** Expression of Actn2 and Aldoa protein in rat skin; **(e)** Expression of Aloda and CFD protein in control and AMSC-exos-treated (80 μg//mL, 24 hours) in L929 cells. Data present means ± SD of at least 3 independent experiments. *P < 0.05 as compared with model group (control).

well as augment the retention of exosomes *in vivo* [23, 24]. Furthermore, the chitin hydrogel can built an immune-isolation barrier to protect the exosomes from clearance by the host's immune system [25–28]. The results of this study proved the beneficial effect of AMSC-exos-loaded β-ChNF hydrogel on wound healing, which brought new possibilities to explore the promoting wound healing method.

In order to further clarify the promotion mechanism of AMSC-exos-loaded β-ChNF hydrogel on

wound healing, experiments *in vitro* and *in vivo* were conducted. In the absence of known targets, transcriptome and proteomics analysis can be used to study the mechanism of an intervention [29]. After the intervention of AMSC-exos-loaded β-ChNF hydrogel, we found the changes in 18 genes and 169 proteins based on transcriptome and proteomics. According to the combined analysis results, we paid attention to the changes of CFD and downstream Aldoa and Actn2 proteins, and the PPI analysis clarified the protein interaction relationship. CFD is widely involved in pathophysiological responses and immune regulation in the body. Its abnormal activation will release a large number of inflammatory factors and cause damage to the body. In addition, it was found that senescent cells promoted the degradation of fibroblast-derived extracellular matrix near the dermis through the secretion of CFD [30, 31]. Thus, proper regulations of the complement system may provide proactive strategies in injury-related diseases, which are also proved by our results during wound healing [32, 33].

Aldolase A, which is an interacting protein of CFD, is ubiquitously distributed in all organs and//or cells, and plays an essential role in glycolytic ATP biosynthesis. Although the vast majority of nonproliferation differentiated cells use oxidative phosphorylation for ATP production in the normal tissue, Aldoa plays an important role in cell proliferation [34–36]. Recently, it has been reported that Aldoa overexpression can increase the cell-cell adhesion-related proteins and promote cell migration by decreasing E-cadherin and β-catenin [37]. To further prove the mechanism of AMSC-exos-loaded β-ChNF hydrogel during wound healing, we detected the effect of AMSC-exos intervention on CFD and downstream Aldoa proteins expression in L929 cells. The results showed that AMSC-exos could significantly decrease the level of CDF and promote the expression of Aldoa protein in L929 cells. The expression of CFD and downstream Aldoa proteins are related to the effect of AMSC-exos-loaded β-ChNF hydrogel on wound healing.

In conclusion, we found that AMSC-exos could promote fibroblasts' proliferation at the doses of 80 and 160 μg/mL, and the effects are related to CFD and downstream Aldoa proteins. AMSC-exos-loaded β-ChNF hydrogel was successfully constructed and improved the application effects of exosomes during wound healing. Based on transcriptomics and proteomics, the changes of related genes and proteins were found and verified by ELISA and Western blotting. These results provide a theoretical basis for the further understanding of exosomes' role in wound healing, and AMSC-exos-loaded β-ChNF hydrogel may be applied as a new therapeutic approach for wound healing.

Authors' contributions

HX J, YL B and YE L designed the experiments. Y Z and MX H provided guidance. Y L wrote the manuscript. RF Z, S M, and PF C performed the experiments. M W completed the statistical analysis. All the authors read and approved the final manuscript.

Ethical considerations

The animal use protocol listed below has been reviewed and approved by the Animal Ethical and Welfare Committee. Approval No. BLB19J012.

Conflict of interests

The authors declare that we have no known competing financial interests or personal relationships that could have appeared to influence the work reported in this paper.

References

1. Zhang B, Wang M, Gong A, et al. HucMSC-Exosome Mediated-Wnt4 Signaling Is Required for Cutaneous Wound Healing. Stem Cells. 2015; 33(7): 2158–2168, doi: 10.1002/stem.1771, indexed in Pubmed: 24964196.
2. Li J, Chen L, Xu J, et al. Effects of Periploca forrestii Schltr on wound healing by Src meditated Mek/Erk and PI3K/Akt signals. J Ethnopharmacol. 2019; 237: 116–127, doi: 10.1016/j.jep.2019.03.046, indexed in Pubmed: 30905787.
3. Yu M, Liu W, Li J, et al. Exosomes derived from atorvastatin-pretreated MSC accelerate diabetic wound repair by enhancing angiogenesis via AKT/eNOS pathway. Stem Cell Res Ther. 2020; 11(1): 350, doi: 10.1186/s13287-020-01824-2, indexed in Pubmed: 32787917.
4. Oh M, Lee J, Kim YuJ, et al. Exosomes derived from human induced pluripotent stem cells ameliorate the aging of skin fibroblasts. Int J Mol Sci. 2018; 19(6), doi: 10.3390/ijms19061715, indexed in Pubmed: 29890746.
5. Cooper DR, Wang C, Patel R, et al. Human adipose-derived stem cell conditioned media and exosomes containing promote human dermal fibroblast migration and ischemic wound healing. Adv Wound Care (New Rochelle). 2018; 7(9): 299–308, doi: 10.1089/wound.2017.0775, indexed in Pubmed: 30263873.
6. Zhang K, Zhao X, Chen X, et al. Enhanced therapeutic effects of mesenchymal stem cell-derived exosomes with an injectable hydrogel for hindlimb ischemia treatment. ACS Appl

Mater Interfaces. 2018; 10(36): 30081–30091, doi: 10.1021/acsami.8b08449, indexed in Pubmed: 30118197.

7. Wang C, Wang M, Xu T, et al. Engineering bioactive self-healing antibacterial exosomes hydrogel for promoting chronic diabetic wound healing and complete skin regeneration. Theranostics. 2019; 9(1): 65–76, doi: 10.7150/thno.29766, indexed in Pubmed: 30662554.

8. Shi Q, Qian Z, Liu D, et al. GMSC-Derived Exosomes Combined with a Chitosan/Silk Hydrogel Sponge Accelerates Wound Healing in a Diabetic Rat Skin Defect Model. Front Physiol. 2017; 8: 904, doi: 10.3389/fphys.2017.00904, indexed in Pubmed: 29163228.

9. Nooshabadi VT, Khanmohamadi M, Valipour E, et al. Impact of exosome-loaded chitosan hydrogel in wound repair and layered dermal reconstitution in mice animal model. J Biomed Mater Res A. 2020; 108(11): 2138–2149, doi: 10.1002/jbm.a.36959, indexed in Pubmed: 32319166.

10. Shafei S, Khanmohammadi M, Heidari R, et al. Exosome loaded alginate hydrogel promotes tissue regeneration in full-thickness skin wounds: An in vivo study. J Biomed Mater Res A. 2020; 108(3): 545–556, doi: 10.1002/jbm.a.36835, indexed in Pubmed: 31702867.

11. Wan ACA, Tai BCU. CHITIN - a promising biomaterial for tissue engineering and stem cell technologies. Biotechnol Adv. 2013; 31(8): 1776–1785, doi: 10.1016/j.biotechadv.2013.09.007, indexed in Pubmed: 24080076.

12. Choi EW, Seo MK, Woo EY, et al. Exosomes from human adipose-derived stem cells promote proliferation and migration of skin fibroblasts. Exp Dermatol. 2018; 27(10): 1170–1172, doi: 10.1111/exd.13451, indexed in Pubmed: 28940813.

13. Zhao G, Liu F, Liu Z, et al. MSC-derived exosomes attenuate cell death through suppressing AIF nucleus translocation and enhance cutaneous wound healing. Stem Cell Res Ther. 2020; 11(1): 174, doi: 10.1186/s13287-020-01616-8, indexed in Pubmed: 32393338.

14. Borges GÁ, Elias ST, da Silva SM, et al. In vitro evaluation of wound healing and antimicrobial potential of ozone therapy. J Craniomaxillofac Surg. 2017; 45(3): 364–370, doi: 10.1016/j.jcms.2017.01.005, indexed in Pubmed: 28169044.

15. Chen L, Jiang P, Li J, et al. Periplocin promotes wound healing through the activation of Src/ERK and PI3K/Akt pathways mediated by Na/K-ATPase. Phytomedicine. 2019; 57: 72–83, doi: 10.1016/j.phymed.2018.12.015, indexed in Pubmed: 30668325.

16. Ma T, Fu B, Yang X, et al. Adipose mesenchymal stem cell-derived exosomes promote cell proliferation, migration, and inhibit cell apoptosis via Wnt/β-catenin signaling in cutaneous wound healing. J Cell Biochem. 2019; 120(6): 10847–10854, doi: 10.1002/jcb.28376, indexed in Pubmed: 30681184.

17. Jiang Z, Li L, Li H, et al. Preparation, biocompatibility, and wound healing effects of O-carboxymethyl chitosan nonwoven fabrics in partial-thickness burn model. Carbohydr Polym. 2022; 280: 119032, doi: 10.1016/j.carbpol.2021.119032, indexed in Pubmed: 35027134.

18. Chen L, Jiang P, Li J, et al. Periplocin promotes wound healing through the activation of Src/ERK and PI3K/Akt pathways mediated by Na/K-ATPase. Phytomedicine. 2019; 57: 72–83, doi: 10.1016/j.phymed.2018.12.015, indexed in Pubmed: 30668325.

19. Zhang W, Bai X, Zhao B, et al. Cell-free therapy based on adipose tissue stem cell-derived exosomes promotes wound healing via the PI3K/Akt signaling pathway. Exp Cell Res. 2018; 370(2): 333–342, doi: 10.1016/j.yexcr.2018.06.035, indexed in Pubmed: 29964051.

20. Lei Z, Singh G, Min Z, et al. Bone marrow-derived mesenchymal stem cells laden novel thermo-sensitive hydrogel for the management of severe skin wound healing. Mater Sci Eng C Mater Biol Appl. 2018; 90: 159–167, doi: 10.1016/j.msec.2018.04.045, indexed in Pubmed: 29853078.

21. Shabbir A, Cox A, Rodriguez-Menocal L, et al. Mesenchymal stem cell exosomes induce proliferation and migration of normal and chronic wound fibroblasts, and enhance angiogenesis in vitro. Stem Cells Dev. 2015; 24(14): 1635–1647, doi: 10.1089/scd.2014.0316, indexed in Pubmed: 25867197.

22. Hu X, Zhou X, Li Y, et al. Application of stem cells and chitosan in the repair of spinal cord injury. Int J Dev Neurosci. 2019; 76: 80–85, doi: 10.1016/j.ijdevneu.2019.07.005, indexed in Pubmed: 31302172.

23. Tao SC, Guo SC, Li M, et al. Chitosan wound dressings incorporating exosomes derived from microrna-126-overexpressing synovium mesenchymal stem cells provide sustained release of exosomes and heal full-thickness skin defects in a diabetic rat model. Stem Cells Transl Med. 2017; 6(3): 736–747, doi: 10.5966/sctm.2016-0275, indexed in Pubmed: 28297576.

24. Rao F, Zhang D, Fang T, et al. Exosomes from human gingiva-derived mesenchymal stem cells combined with biodegradable chitin conduits promote rat sciatic nerve regeneration. Stem Cells Int. 2019; 2019: 2546367, doi: 10.1155/2019/2546367, indexed in Pubmed: 31191669.

25. Azuma K, Koizumi R, Izawa H, et al. Preparation and biomedical applications of chitin and chitosan nanofibers. J Biomed Nanotechnol. 2014; 10(10): 2891–2920, doi: 10.1166/jbn.2014.1882, indexed in Pubmed: 25992423.

26. Khayambashi P, Iyer J, Pillai S, et al. Hydrogel encapsulation of mesenchymal stem cells and their derived exosomes for tissue engineering. Int J Mol Sci. 2021; 22(2): 684, doi: 10.3390/ijms22020684, indexed in Pubmed: 33445616.

27. Ahmad SI, Ahmad R, Khan MS, et al. Chitin and its derivatives: Structural properties and biomedical applications. Int J Biol Macromol. 2020; 164: 526–539, doi: 10.1016/j.ijbiomac.2020.07.098, indexed in Pubmed: 32682975.

28. Jones M, Kujundzic M, John S, et al. Crab vs. Mushroom: a review of crustacean and fungal chitin in wound treatment. Mar Drugs. 2020; 18(1): , doi: 10.3390/md18010064, indexed in Pubmed: 31963764.

29. Bailey-Steinitz LJ, Shih YH, Radeke MJ, et al. An in vitro model of chronic wounding and its implication for age-related macular degeneration. PLoS One. 2020; 15(7): e0236298, doi: 10.1371/journal.pone.0236298, indexed in Pubmed: 32701996.

30. McCullough RL, McMullen MR, Sheehan MM, et al. Complement Factor D protects mice from ethanol-induced inflammation and liver injury. Am J Physiol Gastrointest Liver Physiol. 2018; 315(1): G66–G79, doi: 10.1152/ajpgi.00334.2017, indexed in Pubmed: 29597356.

31. Ezure T, Sugahara M, Amano S. Senescent dermal fibroblasts negatively influence fibroblast extracellular matrix-related gene expression partly via secretion of complement factor D. Biofactors. 2019; 45(4): 556–562, doi: 10.1002/biof.1512, indexed in Pubmed: 31026383.

32. Qi H, Wei J, Gao Y, et al. Reg4 and complement factor D prevent the overgrowth of E. coli in the mouse gut. Commun Biol. 2020; 3(1): 483, doi: 10.1038/s42003-020-01219-2, indexed in Pubmed: 32879431.

33. Song NJ, Kim S, Jang BH, et al. Small molecule-induced complement factor d (adipsin) promotes lipid accumulation and adipocyte differentiation. PLoS One. 2016; 11(9): e0162228, doi: 10.1371/journal.pone.0162228, indexed in Pubmed: 27611793.

34. Wang C, Xu J, Yuan D, et al. Exosomes carrying ALDOA and ALDH3A1 from irradiated lung cancer cells enhance migration and invasion of recipients by accelerating glycolysis. Mol Cell Biochem. 2020; 469(1-2): 77–87, doi: 10.1007/s11010-020-03729-3, indexed in Pubmed: 32297178.

35. Chang YC, Chan YC, Chang WM, et al. Feedback regulation of ALDOA activates the HIF-1α/MMP9 axis to promote lung cancer progression. Cancer Lett. 2017; 403: 28–36, doi: 10.1016/j.canlet.2017.06.001, indexed in Pubmed: 28610954.

36. Lincet H, Icard P. How do glycolytic enzymes favour cancer cell proliferation by nonmetabolic functions? Oncogene. 2015; 34(29): 3751–3759, doi: 10.1038/onc.2014.320, indexed in Pubmed: 25263450.

37. Saito Y, Takasawa A, Takasawa K, et al. Aldolase A promotes epithelial-mesenchymal transition to increase malignant potentials of cervical adenocarcinoma. Cancer Sci. 2020; 111(8): 3071–3081, doi: 10.1111/cas.14524, indexed in Pubmed: 32530543.

Submitted: 26 December, 2021
Accepted after reviews: 21 May, 2022
Available as AoP: 30 May, 2022